

Ethylene/1-Hexene Copolymerization and Synthesis of LLDPE/Nanocarbon Composite through In Situ Polymerization^{1, 2}

Nikoo Nabizadeh^a, Gholam Hossein Zohuri^{a,*}, Mostafa Khoshsefat^b,
Navid Ramezani^a, and Saeid Ahmadjo^b

^aDepartment of Chemistry, Faculty of Science, Ferdowsi University of Mashhad, Mashhad, Iran

^bDepartment of Catalyst, Iran Polymer and Petrochemical Institute, Tehran, Iran

*e-mail: zohuri@um.ac.ir

Received April 7, 2017;

Revised Manuscript Received July 21, 2017

Abstract—Copolymerization of ethylene/1-hexene using a modified ZN-type catalyst was carried out in the presence of triethylaluminium as cocatalyst. The optimum copolymerization activity was obtained at Al : Ti = 357 : 1, 60°C and the comonomer concentration of 0.6 mol/L in the range studied. Copolymer/nanocarbon (including multiwalled carbon nanotube, graphene nanoplatelet) composites were prepared via in-situ polymerization. The copolymerization activity decreased by addition of the nanocarbon into the reactor. The presence of graphene nanoplatelet in nanocomposites reduced the melting temperature and increased heat of fusion, crystallinity and density of the obtained polymer. In the copolymer/carbon nanotube nanocomposites, decreasing of melting temperature was observed in comparison to pure copolymer, whereas, heat of fusion, crystallinity and density increased. The results of TGA analysis showed that the addition of nanocarbons has improved the thermal stability of obtained copolymers.

DOI: 10.1134/S1560090418010104

INTRODUCTION

Nowadays, polyolefins play an important role in many applications, particularly linear low-density polyethylene (LLDPE). LLDPE is very attractive polymer due to its excellent properties, such as low density, good mechanical properties, easy fabrication and recycling [1–3]. LLDPE is a copolymer of ethylene with C₄–C₈ α-olefins. Because it contains a small amount of short-chain branches along the backbone of polymer chains, the crystallinity, melting temperature, and density are lower than for ethylene homopolymer. Introduction of α-olefin comonomer into the polyethylene chain alters the structure, and consequently the properties of the polymer product obtained. This effect is dependent on the type of catalytic system used, polymerization conditions as well as the comonomer type that is introduced [4–8].

Among all of PE grades, the LLDPE offers many interesting properties; however, its relatively low creep resistance, barrier of oxygen, poor stiffness and electrical conductivity may limit its application in some fields. Based on this, addition of small amounts of nanoparticles have proved to play a beneficial role in

improving of its applications in packaging, electronics industries, etc. [9–14].

Synthesis of nanocomposites can be carried out by three main methods; in situ polymerization, solution and melt mixing [14–19]. Among these methods, in situ polymerization is one of the most promising and efficient methods to synthesize polyolefin nanocomposites [14]. The nanocarbons such as carbon nanotube, graphene nanoplatelets, etc. with their striking features of the polymer properties have captured attention of numerous researchers. For instance, Kaminsky et al. used multi-walled carbon nanotubes (CNTs) through in situ polymerization method for ethylene and propylene homopolymerization. Activities of single site metallocene catalysts decreased as the percentage of nanotubes increased. They also observed increasing in crystallization temperature and variations in molecular weight polyethylene and polypropylene composites. Moreover, the presence of CNTs in polymer matrices resulted in a significant improvement in electrical conductivity as well as improved mechanical strength [20]. Boggioni synthesized ethylene-co-norbornene copolymers grafted CNTs composites by in situ polymerization in the presence of Ti-based catalyst and MAO as co-catalyst. Based on the results, the grafted CNTs caused increasing in glass transition temperature and Young's modulus in comparison neat ethylene/norbornene copolymer [21].

¹ The article is published in the original.

² Supplementary materials are available for this article at 10.1134/S1560090418010104 and are accessible for authorized users.

Similarly, some reports have described the application of nanocarbons in the synthesis of polyethylene and polypropylene by metallocene catalysts [22–26]. Beneficial influence of CNTs on the productivity, increasing in polymer molecular weights, degradation temperature, some mechanical and electrical properties have been described. Moreover, the presence of graphene in the catalytic system caused to decreasing in catalyst activity, polymer crystallinity and increasing of M_w , mechanical and electrical properties [25, 26]. A series of Ni-based late transition metal catalysts were anchored on the MWCNTs with amido linkage. According to the report, they achieved good dispersion of the MWCNTs along with an increasing in both catalyst activity and M_w of the polyethylene due to the heterogenized system in presence of CNTs [27]. Cheng, Liu, and Wang also used CNTs and graphene as support for Ziegler-Natta catalysts for polymerization of ethylene and propylene. Increasing of catalyst productivity, mechanical and thermal properties and isotacticity index were some of their presented results [28–30]. There are also some reports, which presented the synthesis of LLDPE/nanocarbon composites by in situ polymerization. For instance, Dubois et al. used a tandem catalysts system including early–late transition metal complexes for the preparation of multiwalled carbon nanotubes (MWCNTs) coated with structurally tailored LLDPE [31]. Casagrande and et al. prepared LLDPE composites using different types of nanofiller (TiO_2 , MWCNT, expanded graphite, and boehmite) in the presence of a tandem catalyst system. Thermal and mechanical properties of the prepared nanocomposites were various. Decreasing of catalyst activities, the ability of MWCNT to nucleate LLDPE crystallization and inferior mechanical properties of LLDPE/EG were the highlighted results of the report [32]. Al-Harhi reported nanocomposites preparation by in situ polymerization of ethylene and graphene. Presence of graphene caused decreasing in catalyst activity, polyethylene crystallinity and increasing of M_w , storage and loss moduli of the material [26].

In this study, the influence of the reaction conditions on the copolymerization of ethylene and 1-hexene using Ziegler Natta catalyst was investigated. Moreover, MWCNTs and graphene nanoplatelets were used in synthesis of LLDPE/nanocarbon composites through the in situ polymerization. Catalyst performance along with some microstructural, thermal and morphological properties of copolymer and nanocomposites are further discussed.

EXPERIMENTAL

Materials

All chemicals and catalyst preparation were kept and manipulated under an argon atmosphere using a glove box and/or Schlenk techniques. Ethylene

(polymerization grade, 99.5%) and argon (99.99%) were supplied by Maron Petrochemical Co. and Roham gas Co., respectively. The chemicals were purified by passage through the columns of activated 13 X and 4 Å type molecular sieves. Toluene was purchased from Mojallali Chemical Co, it was dried over calcium hydride and distilled over sodium wire/benzophenone under an argon atmosphere and stored over activated 13 X/4 Å types molecular sieves for further drying before use. 1-Hexene (98%) purchased from Merck Chemical Co. was purified by distillation over sodium wire, and stored in a Schlenk flask containing 4 Å molecular sieves under high purity nitrogen atmosphere. Triethylaluminium (TEA), (93%) as co-catalyst was supplied by Aldrich Chemical Co. and was diluted using toluene to 1M prior to use. Ziegler Natta catalyst was used for copolymerization with a Ti content of 2.8 wt%. Multiwall carbon nanotube (MWCNT 20–30 nm, MWCNT 30–50 nm) and graphene nanoplatelet (GnP) were supplied by XG Sciences.

The catalyst was prepared according to our previous report [33]. The $\text{TiCl}_4/\text{MgCl}_2 \cdot n\text{EtOH}/\text{DIBP}$ which contained 2.8 wt% of Ti was used for copolymerization.

Copolymer and Nanocomposite Synthesis

Copolymerization of ethylene and 1-hexene was carried out in a 100 mL, two-necked round-bottom flask which was equipped with ethylene inlet, and magnetic stirrer, while at high pressure of ethylene (more than 2 bars), it was carried out using a 1-l Buchibmd 300-type stainless steel reactor. The monomer, co-catalyst and catalyst were introduced to reactor, respectively. At the end of the polymerization, the reaction was quenched and copolymer was precipitated by adding acidified methanol (10%). The obtained product was filtered, washed and dried under vacuum at 40°C. In the in-situ polymerization, a specific amount of nanoparticles was stirred for 15 min with catalyst prior to injection into the reactor.

Characterization

Melting temperature T_m and enthalpy of fusion ΔH_m of the copolymer were determined with a Mettler Toledo DSC 822e scanning calorimeter. Indium was used for the calibration of the temperature scale. The melting endotherms were measured during reheating of the polymer sample (5 mg) to 250 or 300°C at a heating rate of 10 deg/min under nitrogen flow. Calculation of $\Delta H_m/\Delta H_m^* \times 100$ gives the degree of crystallinity, where ΔH_m is the heat of melting sample (J/g) and ΔH_m^* is the heat of melting of polyethylene with 100% crystallinity (J/g) [34, 35]. The relation of ΔH_m

Table 1. Copolymerization of ethylene/1-hexene at the different reaction conditions

No	Ethylene pressure, bar	[1-hexene], mol/L	[Al]/[Ti]	t_p , min	T_p , °C	Yield, g	Activity $\times 10^5$ g copolymer/mol cat.h
1	1	0.6	107	60	60	0.022	0.007
2	1	0.6	286	60	60	2.000	0.715
3	1	0.6	357	60	60	5.110	1.830
4	1	0.6	428	60	60	1.500	0.536
5	1	0.6	536	60	60	0.89	0.320
6	1	0.6	357	60	50	3.33	1.20
7	1	0.6	357	60	70	2.7	0.96
8	1	0.6	357	5	60	1.14	5.00
9	1	0.6	357	15	60	2.00	2.80
10	1	0.6	357	30	60	2.88	2.00
11	1	0.6	357	120	60	7.00	1.2
12	0.5	0.6	357	60	60	6.50	1.3
13	1.5	0.6	357	60	60	5.11	1.8
14	3	0.6	357	60	60	4.52	2.0
15	5	0.6	357	60	60	3.85	2.3
16	1	0	357	60	60	4.45	0.79
17	1	0.22	357	60	60	5.00	0.90
18	1	1.30	357	60	60	5.9	1.00
19	1	1.70	357	60	60	4.63	0.80

Copolymerization conditions: [Ti] = 28×10^{-3} mmol, Triethylaluminum as co-catalyst, Toluene = 35 mL.

(J/g) to the copolymer density d was obtained through the following semi empirical Eq. (1) [36]:

$$d = (2195 + \Delta H_m)/2500. \quad (1)$$

FTIR spectra were recorded by Thermo Nicolet Avatar 370 FTIR spectrograph. The spectra were obtained in the standard wave number range from 4000 to 400 cm^{-1} . To determine the vinyl group concentration, the area under the absorbance band for the vinyl CH group at 908 cm^{-1} and the area under the reference polyethylene absorbance band at 2019 cm^{-1} were measured. The Number C=C per 1000 C atoms ($N_{C/1000}$) was calculated according to the following Eq. (2) [37]:

$$N_{C/1000} = 2.751 \times [A_{908}/A_{2019}] - 0.111. \quad (2)$$

SEM analysis was conducted to study the morphologies of the copolymers. Morphological study of the copolymer was carried out using LEO VP1450 SEM in Ferdowsi university of Mashhad. The M_n of the samples was determined by an Ubbelohde viscometer in decaline at $133 \pm 1^\circ\text{C}$ using Mark-Houwink constant values equal to 0.70 and 0.062 (mL/g) for polyethylene by Eq. (3) [38]:

$$[\eta] = KM_n^\alpha. \quad (3)$$

The nanocomposite samples were analyzed by Mettler Toledo STARE TGA, which heated from 25 to

800°C at a constant rate of 10 deg/min. The char yield can be an effective parameter to estimate the limited oxygen index (LOI) according to the Van Krevelen-Hoftyzer's Eq. (4) [39] where the CR is the char yield.

$$\text{LOI} = 17.5 + 0.4 \text{ CR}. \quad (4)$$

RESULTS AND DISCUSSION

Influence of the Polymerization Conditions on the Catalyst Activity

The co-catalyst, triethylaluminum (TEA), can act as a scavenger to remove impurities and regeneration of the active sites. In general, copolymerization kinetic strongly depends on co-catalyst concentration. Based on this, the effect of Al : Ti molar ratios on the copolymerization of ethylene with 1-hexene was studied. The results are shown in Table 1. It was observed that the optimum molar ratio of Al : Ti was at 357 : 1 (entry 3). Briefly, the catalyst activity for copolymerization initially increased to a maximum value and then decreased at higher amount of TEA.

One possible interpretation for the maximum rate at a certain co-catalyst concentration is competitive adsorption between monomer and co-catalyst on the same active site, which can be attributed to the change of catalyst active sites [4, 40]. It also has been demonstrated that the co-catalyst in low concentrations, pre-

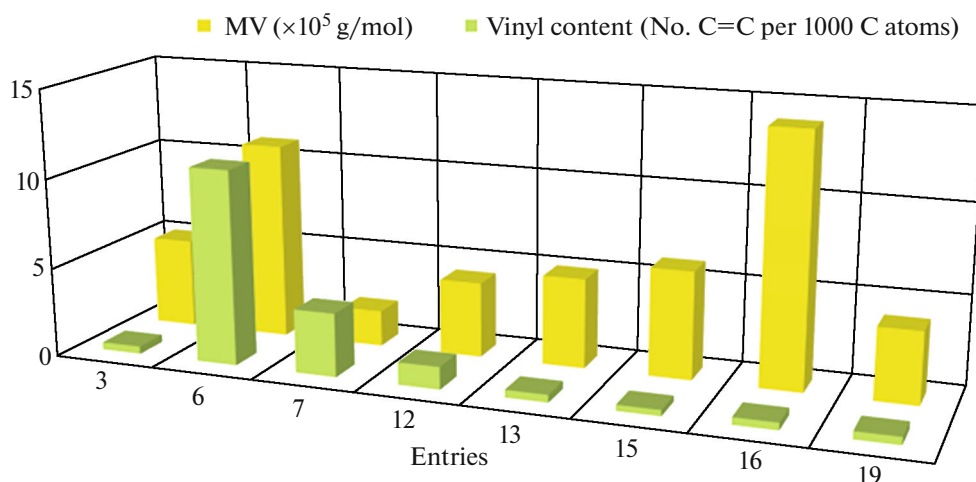


Fig. 1. (Color online) The viscosity average molecular weights M_{η} and vinyl contents of various copolymerization run. Here and below polymerization conditions are given in Table 1.

clude activation of the optimal active centers, while higher concentrations inflict over-reduction of Ti^{+4} to Ti^{+2} , which leads to decreasing in the overall catalyst performance [33].

Copolymerization reactions were carried out in the polymerization temperature range of 50–70°C. The optimum temperature at which the catalyst showed the highest activity was 60°C. The influence of copolymerization temperature on the catalyst activity, M_{η} and vinyl content of the synthesized copolymer are shown in Table 1 and Fig. 1 (entries 3, 6 and 7). In the polymerization systems, chain transfer reactions tend to increase by increasing polymerization temperature. It is normally observed that higher initial polymerization rate and much catalyst deactivation are obtained at higher polymerization temperatures [41, 42]. The M_{η} decreased as polymerization temperature raised; it indicates that the propagation/termination rate ratios

decreased which may be a result of chain transfer to aluminum, monomer or β -H elimination reactions at higher polymerization temperatures [33, 43].

The number of unsaturation sites is also fallen to the lowest extent at 60°C. Further increasing of the temperature and reduction of solubility of the monomer lead to more comonomer reaching to active center; as a result, amount of vinyl content increased.

To clarify the effect of copolymerization time (kinetic of copolymerization) on the copolymerization using the supported Ziegler-Natta catalyst, in addition to entries 3, 8, 9, 10, and 11 in Table 1, they are depicted in Fig. 2. During first 5 min of the reaction, the catalyst has reached to the highest activity. Then degradation, deactivation and encapsulation of the active centers cause to the decrease in catalyst productivity [44].

The catalyst productivity enhanced as ethylene pressure increased due to high concentration of the monomer near the catalyst active centers which led to increasing of olefin trapping and reinsertion of polymer chain (entries 3, 12, 13, 14, 15 in Table 1 and Fig. 1) [44]. The maximum activity of copolymerization was obtained at the comonomer concentration of 0.6 mol/L (entry 3). Increasing of catalyst productivity can be due to the fragmentation of the catalyst, site activation and better diffusion of ethylene along with incorporation of comonomer. This disrupts PE crystallinity, thereby opening up the polymer surrounding the active sites to allow better ethylene transport to the active sites known as comonomer effect [45]. Two other explanations of comonomer effect (fragmentation and site activation) also can be considered, which describe that presence of the comonomer may enhance the fragmentation, migratory insertion and polymerization rate [45]. Deactivation of active sites and increasing of chain transfer reaction are two possible

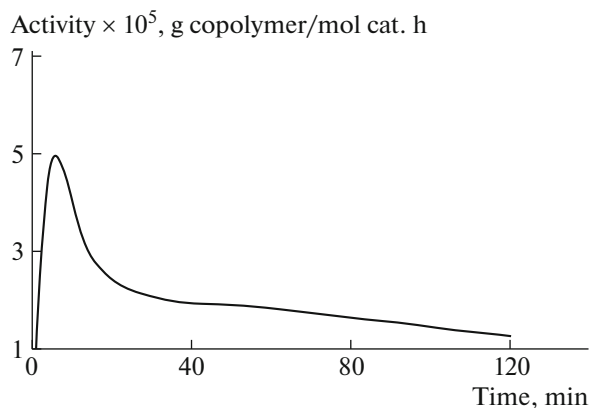


Fig. 2. The effect of the time on copolymerization of ethylene and 1-hexene.

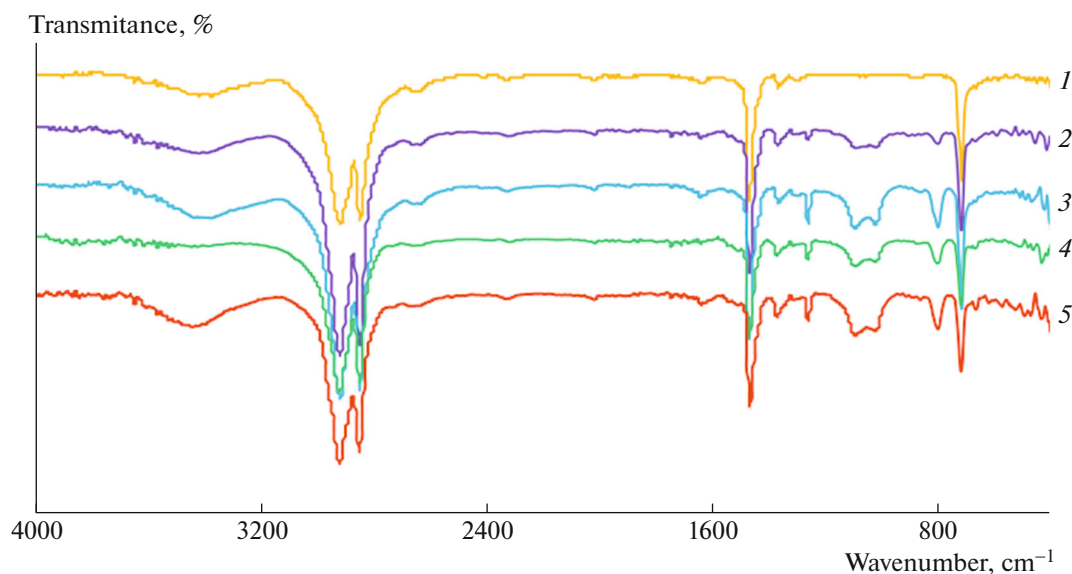


Fig. 3. (Color online) FTIR spectra of PE and LLDPE samples: entry (1) 16, (2) 17, (3) 3, (4) 18, and (5) 19.

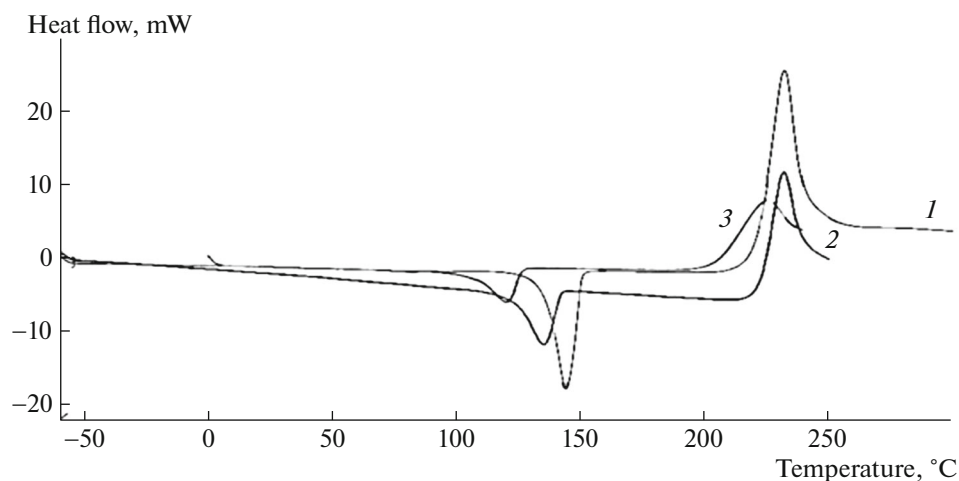


Fig. 4. DSC analysis of (1) polyethylene (entry 16), (2) copolymer (entry 3) and (3) copolymer (entry 19).

reasons of decreasing of catalyst performance and copolymer molecular weight at higher concentration of comonomer [44].

As it can be observed in Fig. 3, the intensity of bands assigned to the chain branches, which increased as comonomer concentration augmented in the feed. Four characteristic bands of polyethylene were observed at 2917, 2849, 1471 and 718 cm^{-1} . There was also a sharp band at 1372 cm^{-1} that is related to the branches. The band intensities enhanced with increasing of comonomer incorporation (see Fig. 3).

Decreasing of melting temperature, crystallinity extent and density of polyethylene by introducing of comonomer in the polymer chain can be observed in Fig. 4. The melting points dropped off from 143°C (neat

PE, entry 16) to 134 and 133 for entries 3 and 19, respectively. Moreover, crystallinity extent decreased from 64.5% for neat polyethylene (entry 16) to 33.5 and 20.3% correspond to entries 3 and 19. The densities of samples calculated using equation (1) indicated that by comonomer incorporation into polyethylene chain, density decreased from 0.95 to 0.92 and 0.90 g/cm^3 .

LLDPE/Nanocarbon Nanocomposites

The effects of nanocarbons on the copolymerization activity of catalyst and melting point, crystallinity, density and vinyl content of polymer are shown in Table 2 (FTIR spectra are given in supporting information; Figs. S11–S16). By increasing of GnP and MWCNTs, activity of the catalyst in copolymerization

Table 2. LLDPE/MWCNT and LLDPE/graphene nanocomposites synthesis

No	Nanocarbon	Yield	Nano-carbon, %	Activity $\times 10^5$ g copolymer/mol cat. h	T_m , °C	ΔH_m , J/g	X_c , %	D , g/mL	Vinyl content (C=C/1000 C)
3	0	7.00	0	1.25	134	97.20	33.50	0.917	0.43
20	10 mg GnP	4.10	0.25	0.70	132	118.90	41	0.925	0.38
21	30 mg GnP	2.90	1.03	0.50	—	—	—	—	—
22	10 mg MWCNT _{20–30}	3.85	0.26	0.70	132	114.10	39.34	0.924	0.39
23	30 mg MWCNT _{20–30}	1.72	1.74	0.30	—	—	—	—	—
24	10 mg MWCNT _{30–50}	3.95	0.25	0.72	129	86.30	29.75	0.912	0.75
25	30 mg MWCNT _{30–50}	1.85	1.62	0.35	—	—	—	—	—

Copolymerization conditions: $[Ti] = 28 \times 10^{-3}$ mmol, $T = 60^\circ\text{C}$, $[Al] : [Ti] = 357 : 1$, $P = 1.5$ bar, $t = 2$ h, $[1\text{-hexene}] = 0.6$ mol/L and toluene = 35 mL.

Table 3. Effect of Graphene and Multi-walled carbon nanotubes on thermal stability, char yield and the limited oxygen index

Entry	Samples	$T_{dg5\%}$, °C	$T_{dg50\%}$, °C	$T_{dg95\%}$, °C	CR, %	LOI
3	LLDPE	425.90	470.50	490.90	0.59	17.736
20	LLDPE/Graphene	436.80	472.00	491.70	0.87	17.848
22	LLDPE/CNT _{20–30 nm}	437.80	476.70	492.50	0.73	17.792
24	LLDPE/CNT _{30–50 nm}	437.30	472.40	492.00	0.76	17.804

was decreased [20, 26, 32]. It can be attributed to some remaining active polar functional groups on the surface of the nanocarbons deactivated the catalyst as in FTIR spectrums it can be observed [25]. It also can be suggested that GnP and MWCNT presumably are barrier for the fragmentation of the catalyst and cause inaccessibility of active sites for the monomers in copolymerization.

The melting temperatures and vinyl contents of copolymers slightly decreased, however they were not affected significantly by the presence of GnP and MWCNT (20–30 nm). While, the crystallinity and density increased as GnP and MWCNT (20–30 nm) both reduced the comonomer incorporation and acted as a nucleating agents [25, 32, 47, 48]. The variation in the densities and crystallinity content related to the size and steric effect of the nanocarbons which in MWCNT (20–30 nm), density and crystallinity decreased in comparison to neat copolymer and the other nanocomposite samples [26, 32].

The morphology of copolymer and nanocomposites were studied using scanning electron microscopy (SEM). By considering SEM images of neat copolymer, nanocarbons caused a significant change in morphology of polymer. As it can be observed (Fig. 5), the diameters of nanocomposites were 270–880 nm for copolymer/MWCNT (30–50 nm) and 260–400 nm for copolymer/MWCNT (20–30 nm). Further SEM

images (magnification ranging from 1000 \times to approximately 20,000 \times) are available in the Figs. S17–S112.

Higher thermal stability of nanocomposites was observed in comparison to neat copolymer according to TGA data [14, 49–51]. The results of gravimetric curves (Figs. S113–S116) showed that the addition of nanocarbons improved the thermal stability of copolymers from 425.9 to 436.8 $^\circ\text{C}$ in the copolymer/GnP at the beginning of degradation $T_{dg5\%}$, from 470.5 to 472.0 $^\circ\text{C}$ in main degradation of the nanocomposite $T_{dg50\%}$ and from 490.9 to 491.7 $^\circ\text{C}$ at the end of nanocomposite degradation $T_{dg95\%}$. Char yield changes from 0.59 to 0.87 and the limited oxygen index remained stable.

For copolymer/MWCNT (20–30 nm) and copolymer/MWCNT (30–50 nm) samples, the initial degradation temperature changes from 425.9 to 437.8 and 437.3 $^\circ\text{C}$ ($T_{dg5\%}$), respectively. Moreover, the main degradations shifted from 470.50 to 476.7 and to 472.4 $^\circ\text{C}$ ($T_{dg50\%}$), the end of degradation temperature shifted from 490.9 to 492.5 and to 492.0 $^\circ\text{C}$ ($T_{dg95\%}$), respectively. Char yield increased from 0.59 to 0.73 and to 0.76 for MWCNT (20–30 nm) and CNT (30–50 nm), sequentially. The limited oxygen index remained constant.

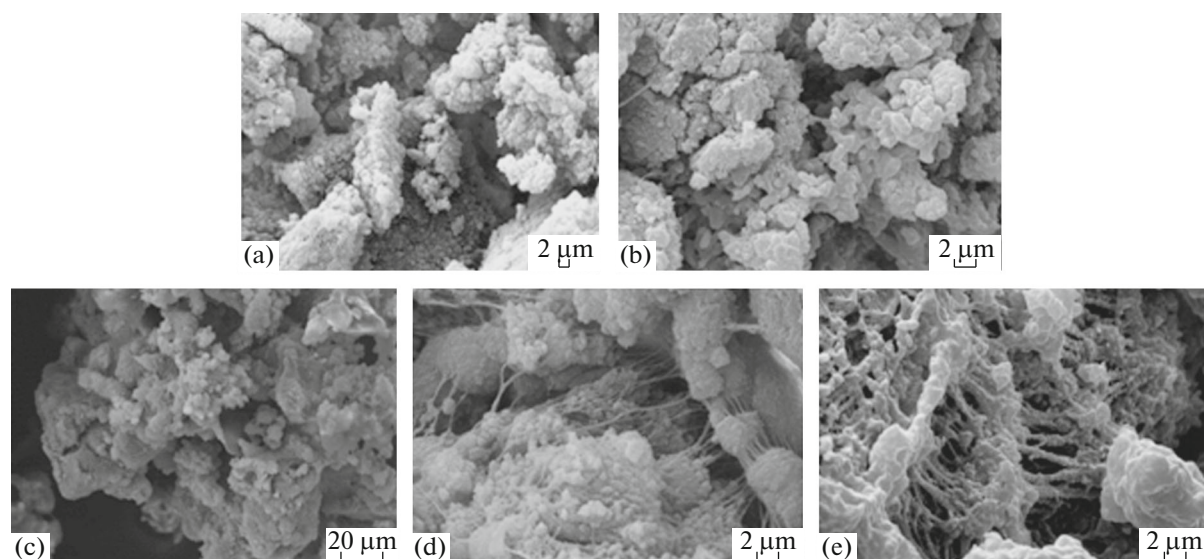


Fig. 5. SEM image of (a) polyethylene, (b) LLDPE (entry 3), (c) LLDPE/GnP composite (entry 20), (d) LLDPE/MWCNT20-30 composite (entry 22), (e) LLDPE/MWCNT30-20 composite (entry 24).

COCNLUSIONS

Ethylene/1-hexene copolymers were produced using Ziegler Natta catalyst and the effects of copolymerization conditions on the copolymer yield were investigated. The results showed that optimum molar ratio of Al : Ti (357 : 1) provides the highest productivity. Increasing monomer pressure from 0.5 to 5 bar causes non-linearly increasing of the catalyst productivity. The copolymerization activity increases with addition of the comonomer concentration from 0.2 to 0.6 mol/L, however, further increasing of the 1-hexene concentration leads to reduction of the activity.

LLDPE/nanocarbon composites were prepared successfully via in-situ polymerization. The copolymerization activity was decreased by addition of the nanocarbon into the reactor. Presence of GnP in LLDPE/GnP nanocomposites reduced the melting point and increased heat of fusion, crystallinity and density of the obtained polymer. In the LLDPE/CNT (20–30 nm), decreasing of melting temperature was observed in comparison to pure copolymer, whereas, heat of fusion, crystallinity and density increased. As well as, in LLDPE/CNT (30–50 nm) all of the thermal parameters decreased. The results of TGA analysis showed that the addition of nanocarbons improves the thermal stability of copolymers from 10 to 12°C.

ACKNOWLEDGMENTS

We are thankful of Ferdowsi university of Mashhad (FUM) and Iran Polymer and Petrochemical Institute for all their cooperation.

REFERENCES

1. S. M. M. Mortazavi, H. Arabi, G. Zohuri, M. Nekoomanesh, and M. J. Ahmadi, *Polym. Int.* **59**, 1258 (2010).
2. K. Czaja, M. Bialek, and A. Utrata, *J. Polym. Sci., Part A: Polym. Chem.* **42**, 2512 (2004).
3. H. S. Cho, D. J. Choi, and W. Y. Lee, *J. Appl. Polym. Sci.* **78**, 2318 (2000).
4. G. H. Zohuri, M. M. Mortazavi, R. Jamjah, and S. Ahmadjo, *J. Appl. Polym. Sci.* **93**, 2597 (2004).
5. H. W. Park, J. S. Chung, S. H. Baeck, and I. K. Song, *J. Mol. Catal. A: Chem.* **255**, 69 (2006).
6. S. Ahmadjo, H. Arabi, G. Zohuri, G. Nejabat, and S. M. M. Mortazavi, *J. Therm. Anal. Calorim.* **116**, 417 (2014).
7. P. S. Chum and K. W. Swogger, *Prog. Polym. Sci.* **33**, 797 (2008).
8. M. Mortazavi, H. Arabi, G. Zohuri, S. Ahmadjo, M. Nekoomanesh, and M. Ahmadi, *Macromol. React. Eng.* **3**, 263 (2009).
9. A. Dorigato, A. Pegoretti, and J. Kolarik, *Polym. Compos.* **31**, 1947 (2010).
10. B. Jongsomjit, J. Panpranot, and P. Praserttham, *J. Mater. Lett.* **61**, 1376 (2007).
11. J. Qian, C.-Y. Guo, H. Wang, and Y. Hu, *J. Mater. Sci.* **42**, 4350 (2007).
12. G. Malucelli, S. Ronchetti, N. Lak, A. Priola, N. T. Dintcheva, and F. P. La Mantia, *Eur. Polym. J.* **43**, 328 (2007).
13. C. Desharun, B. Jongsomjit, and P. Praserttham, *Catal. Commun.* **9**, 522 (2008).
14. M. Khoshsefat, S. Ahmadjo, S. M. M. Mortazavi, and G. H. Zohuri, *RSC Adv.* **6**, 88625 (2016).
15. S. Park, S. W. Yoon, H. Choi, J. S. Lee, W. K. Cho, J. Kim, H. J. Park, W. S. Yun, C. H. Choi, Y. Do, and I. S. Choi, *Chem. Mater.* **20**, 4588 (2008).

16. S. Coiai, D. Prevosto, M. Bertoldo, L. Conzatti, V. Causin, C. Pinzino, and E. Passaglia, *Macromolecules* **46**, 1563 (2013).
17. A. P. Sirocic, A. Rescek, M. Scetar, L. K. Krehula, and Z. Hrnjak-Murgic, *Polym. Bull.* **71**, 705 (2014).
18. L. Zhang, E. Yue, B. Liu, P. Serp, C. Redshaw, W. H. Sun, and J. Durand, *Catal. Commun.* **43**, 227 (2014).
19. Y. Y. Huang and E. M. Terentjev, *Polymer* **4**, 275 (2012).
20. W. Kaminsky, in *Polymer-Carbon Nanotube Composites. Preparation, Properties and Applications*, Ed. by T. McNally and P. Pötschke (Woodhead Publ., Cambridge, UK, 2011), pp. 3-24.
21. L. Boggioni, G. Scalcione, A. Ravasio, F. Bertini, C. D. Arrigo, and I. Tritto, *Macromol. Chem. Phys.* **213**, 627 (2012).
22. X. Dong, L. Wang, L. Deng, J. Li, and J. Huo, *Mater. Lett.* **61**, 3111 (2007).
23. S. Park, H. J. Paik, S. W. Yoon, I. S. Choi, K. B. Lee, D. J. Kim, Y. H. Jung, and Y. Do, *Macromol. Rapid Commun.* **27**, 47 (2006).
24. D. Bonduel, M. Mainil, M. Alexandre, F. Monteverde, and P. Dubois, *Chem. Commun.* **6**, 781 (2005).
25. M. A. Milani, D. González, R. Quijada, N. R. S. Basso, M. L. Cerrada, D. S. Azambuja, and G. B. Galland, *Compos. Sci. Technol.* **84**, 1 (2013).
26. F. Shehzad, M. Daud, and M. A. Al-Harathi, *J. Therm. Anal. Calorim.* **123**, 1501 (2016).
27. L. Zhang, E. Castillejos, P. Serp, W. H. Sun, and J. Durand, *Catal. Today* **235**, 33 (2014).
28. X. Tong, C. Liu, H. M. Cheng, H. Zhao, F. Yang, and X. Zhang, *J. Appl. Polym. Sci.* **92**, 3697 (2004).
29. Z. Liu, M. Yu, J. Wang, F. Li, L. Cheng, J. Guo, Q. Huang, Y. Zhou, B. Zhu, J. Yi, Y. Liu, and W. Yang, *J. Ind. Eng. Chem.* **20**, 1804 (2013).
30. N. Wang, Y. Qin, Y. Huang, H. Niu, J. Y. Dong, and Y. Wang, *Appl. Catal., A* **435**, 107 (2012).
31. A. Toti, G. Giambastiani, Ch. Bianchini, A. Meli, St. Bredeau, Ph. Dubois, D. Bonduel, and M. Claes, *Chem. Mater.* **20**, 3092 (2008).
32. A. C. Pinheiro, A. C. A. Casagrande, and O. L. Casagrande, *J. Polym. Sci., Part A: Polym. Chem.* **52**, 24 (2014).
33. S. Ahmadjo, *Polym. Adv. Technol.* **27**, 1523 (2016).
34. D. J. Blundell, D. R. Beckett, and P. H. Willcocks, *Polymer* **22**, 704 (1981).
35. S. Damavandi, N. Samadieh, S. Ahmadjo, Z. Etemadnia, and G. H. Zohuri, *Eur. Polym. J.* **64**, 3506 (2015).
36. C. Carlini, A. D. Alessio, S. Giaiacopi, R. Po, M. Pracella, A. M. R. Galletti, and G. Sbrana, *Polymer* **48**, 1185 (2007).
37. W. Collins, J. Seelenbinder, and F. Higgins, *Determination of Irganox 1010 in Polyethylene by Infrared Spectroscopy* (Agilent Technologies, Inc., Danbury, CT, 2012).
38. *Polymer Data Handbook*, Ed. by J. E. Mark (Oxford Univ. Press, New York, 1999), pp. 498-500.
39. Kh. Faghihi, M. Ashouri, and A. Feyzi, *J. Mex. Chem. Soc.* **57**, 133 (2013).
40. I. L. Kim, J. H. Kim, and S. I. Woo, *J. Appl. Polym. Sci.* **39**, 837 (1990).
41. I. A. Jaber and W. H. Ray, *J. Appl. Polym. Sci.* **50**, 201 (1993).
42. G. H. Zohuri, M. A. Bonakdar, S. Damavandi, M. Eftekhari, M. Askari, and S. Ahmadjo, *Iran. Polym. J.* **18**, 593 (2009).
43. R. Jamjah, G. H. Zohuri, J. Javaheri, M. Nekoomanesh, S. Ahmadjo, and A. Farhadi, *Macromol. Symp.* **274**, 148 (2008).
44. M. Khoshsefat, G. H. Zohuri, N. Ramezani, S. Ahmadjo, and M. Haghpanah, *J. Polym. Sci., Part A: Polym. Chem.* **54**, 3000 (2016).
45. M. P. McDaniel, E. D. Schwerdtfeger, and M. D. Jensen, *J. Catal.* **314**, 109 (2014).
46. Z. Liu, X. Zhang, H. Huang, J. Yi, W. Liu, W. Liu, H. Zhen, Q. Huang, K. Gao, M. Zhang, and W. Yang, *J. Ind. Eng. Chem.* **18**, 2217 (2012).
47. K. P. Noorunnisa and M. A. A. AlMaadeed, *Mater. Des.* **1**, 63 (2015).
48. A. S. Luyt, J. A. Molefi, and H. Krump, *Polym. Degrad. Stab.* **91**, 1629 (2015).
49. T. Kuila, S. Bose, C. E. Hong, M. E. Uddin, P. Khanra, N. H. Kim, and J. H. Lee, *Carbon* **49**, 1033 (2011).
50. P. N. Khanam, M. A. AlMaadeed, M. Ouederni, E. Harkin-Jones, B. Mayoral, A. Hamilton, and D. Sun, *Vacuum* **130**, 63 (2016).
51. T. Kuila, B. J. Jung, X. F. Yi, and J. H. Lee, *Adv. Mater. Res.* **410**, 152 (2012).